ISSN 1064-2269, Journal of Communications Technology and Electronics, 2015, Vol. 60, No. 5, pp. 436–453. © Pleiades Publishing, Inc., 2015.
Original Russian Text © A.S. Godin, A.B. Tsai, K.N. Klimov, 2015, published in Radiotekhnika i Elektronika, 2015, Vol. 60, No. 5, pp. 468–485.

ELECTRODYNAMICS AND WAVE PROPAGATION

Numerical Electrodynamic Analysis of the External Huygens Cube

A. S. Godin[a], A. B. Tsai[b], and K. N. Klimov[a]

[a] *Research and Production Corporation Lianozovo Electromechanical Plant, Dmitrovskoe shosse 110, Moscow, 127411 Russia*

[b] *Concern Morinformsystem-Agat, Shosse Entuziastov 29, Moscow, 105275 Russia*

e-mail: andrey.godin@gmail.com, const0@mail.ru

Received June 25, 2014

Abstract—The frequency characteristics of the external Huygens cube are numerically simulated and compared with those of the internal Huygens cube. Dependence of the frequency characteristics of the external Huygens cube on the sizes of an air cube is analyzed.

DOI: 10.1134/S1064226915050046

INTRODUCTION

We perform numerical simulation of the frequency characteristics of a Huygens element radiating into open space: the standing wave ratio (SWR), losses, attenuation, and amplification. This enables us to evaluate the limiting characteristics that can be reached in real radiators. The Huygens element is usually understood as a hypothetic radiator corresponding to an infinitesimal element of the front of a linearly polarized electromagnetic wave. The Huygens element is introduced into the antenna theory in connection with the principle of equivalent surface currents (electric and magnetic)—the analog of the Huygens principle in optics [1–3]. The principle of equivalent surface currents consists in the following (Fig. 1): sources of the electromagnetic wave found in region I are surrounded by a closed surface C, and the electromagnetic field in region II is calculated from the values of equivalent electric and magnetic surface currents on the closed surface C. Therefore, the surface C has the inner and outer boundaries. Onto the inner boundary, the electromagnetic wave from sources of electromagnetic radiation found in region I is incident and, from the outer boundary, electromagnetic waves are radiated into the open space. For this reason, the Huygens element must have two inputs: one from the side of region I and the other from the side of region II. The same is clear from the mathematical point of view. The boundary conditions for the Huygens element, which is two-sided surface, must be imposed both on two sides and on the boundary of the Huygens element. An infinitesimal cube simulating the front surface of a plane linearly polarized electromagnetic wave in modeling of the radiation to the open space will be called the ideal external Huygens cube (see Fig. 1).

Let us simulate the frequency characteristics of such an object by the ANSYS HFSS v.15 universal electromagnetic software [4]. Unlike the ideal Huygens cube, the simulated object has finite dimensions, and this object will be called an external Huygens cube. It is worth noting once more that the distinctive feature of the Huygens cube is that the conditions of radiation and absorption of a plane wave are imposed not only from the side of region II but also from the side of region I (see Fig. 1). In addition, boundary conditions (two short-circuited (SC) faces and to open-circuited (OC) faces) are imposed on the other faces of the Huygens cube. Thus, the boundary conditions on such a plane-wave element are specified on all boundaries and the problem on radiation and absorption of electromagnetic waves becomes well-posed.

1. ANALYSIS OF THE EXTERNAL HUYGENS CUBE

We consider a cube A with the dimensions of $1 \times 1 \times 1$ mm in the open space (Fig. 2). The cube A is filled

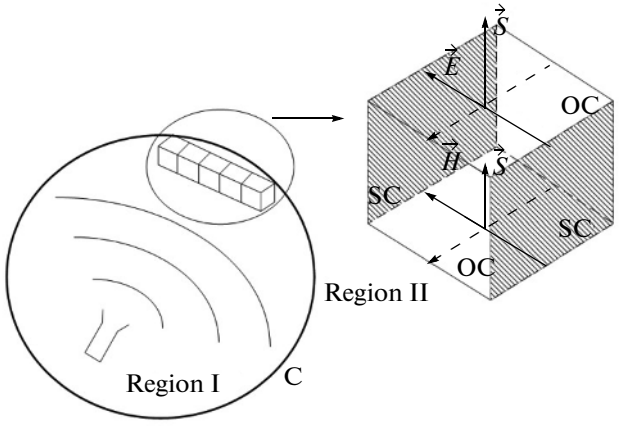

Fig. 1. Illustration of the principle of equivalent surface currents.

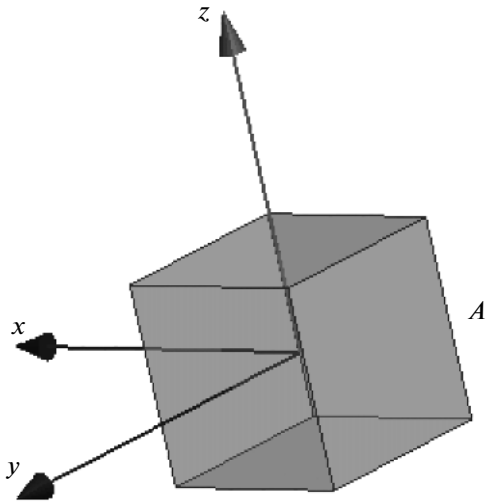

Fig. 2. Geometry of a metal-filled cube *A*.

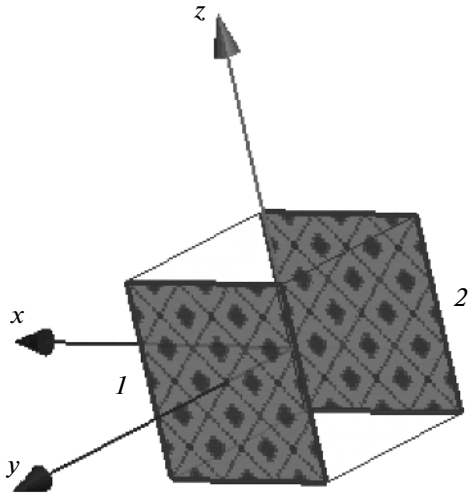

Fig. 3. Short-circuited faces *1* and *2* of cube *A*.

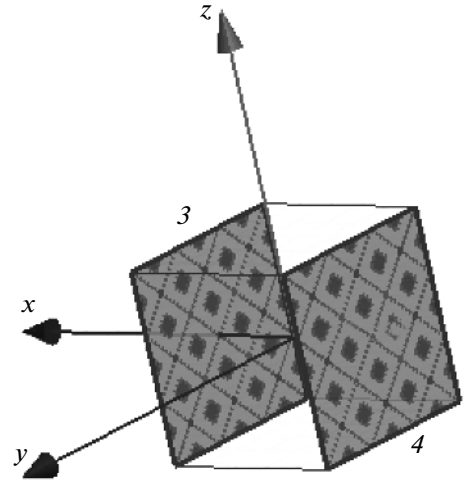

Fig. 4. Open-circuited faces *3* and *4* of cube *A*.

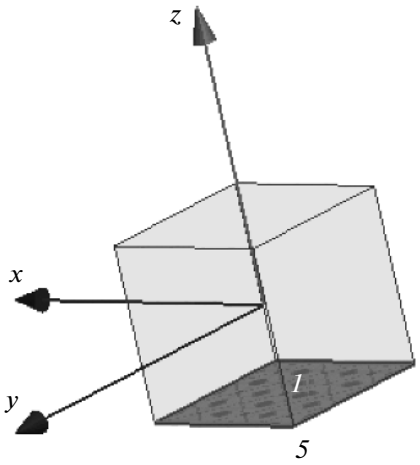

Fig. 5. Face *5* of cube *A*, on which the excitation and matching boundary condition is imposed.

with metal. The tangential electric field E_τ on faces *1* and *2* of the cube *A* (Fig. 3) is set to zero, which corresponds to a metallic wall. Faces *1* and *2* of this cube are assumed to be short-circuited [1–3].

On faces *3* and *4* of the cube *A* (Fig. 4), we set the tangential magnetic field H_τ to zero, which corresponds to a magnetic wall. Faces *3* and *4* of this cube are assumed to be open-circuited [1–3].

On faces *5* and *6* of the cube *A* (Figs. 5, 6), we impose the boundary condition corresponding to the excitation and matching of plane waves [1–3]. Face *5* will be denoted as input *1* (see Fig. 5), and face *6*, as input *2* (see Fig. 6). The polarizations of the electric and magnetic fields and the directions of the Poynting vectors [5–8] of these plane waves are shown in Figs. 7–9.

In order to consider an external electromagnetic problem, we place the proposed geometry of the metal cube *A* with the above-introduced boundary conditions into an air cube *B* (see Fig. 10), on whose faces we impose the radiation conditions [4]. The external air cube *B* has the dimensions 25 × 25 × 25 mm and is vacuum-filled.

Figure 11 shows the faces of cube *B* on which the absorption (radiation) conditions are imposed.

Cube *A* placed into the cube *B* with the absorption (radiation) conditions will be called the external Huygens cube, in contrast to the internal Huygens cube [9].

The problem of electromagnetic-wave scattering in the external Huygens cube was simulated by the ANSYS HFSS v. 15 3D electromagnetic software package [4].

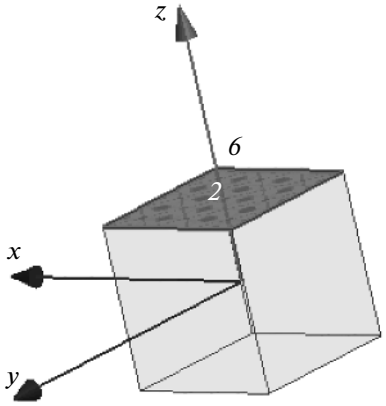

Fig. 6. Face *6* of cube *A*, on which the excitation and matching boundary condition is imposed.

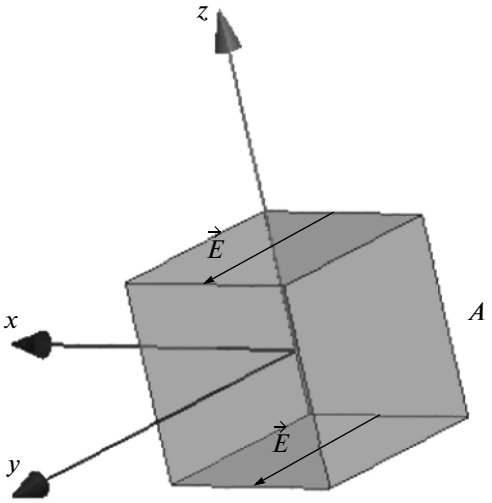

Fig. 7. Directions of the electric field vectors $\vec{E}$ of the waves incident onto faces *5* and *6* of cube *A*.

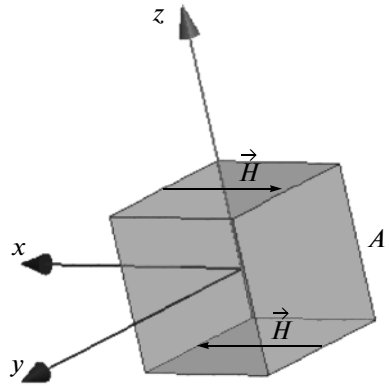

Fig. 8. Directions of the magnetic field vectors $\vec{H}$ of the waves incident onto faces *5* and *6* of cube *A*.

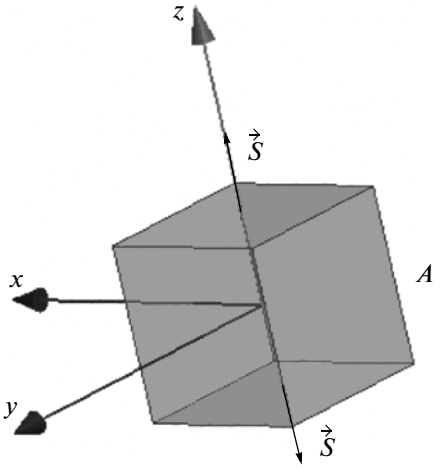

Fig. 9. Directions of the electromagnetic energy flux densities (Poynting vectors) $\vec{S}$ of the waves incident onto faces *5* and *6* of cube *A*.

2. RESULTS OF SIMULATION OF THE EXTERNAL HUYGENS CUBE IN A 25 × 25 × 25 mm AIR BOX

The simulation was performed in a frequency range from 1 to 300 GHz with a step of 5 GHz. The convergence in the moduli of the scattering matrix Delta S was 0.02, the total number of tetrahedra was 228803, the size of the resulting matrix was 1459094, and the required storage was 15.1 GB. The total computation time on a server with two Intel Xeon E5-2690 processors with the frequency of 2.90 GHz and 128 GB RAM was 23 h 13 min 26 s.

Figure 12 shows the frequency characteristic of SWR for the external Huygens cube. Near the frequency of 1 GHz, the side of this cube was of 1/300 of the wavelength, which corresponds to the quasi-static case. Starting from the frequency of 30 GHz, which corresponds to the side of the external Huygens cube of 1/10 of the wavelength, the static components are not sufficient for describing the phenomena inside the cube. Up to 30 GHz (less than 1/10 of the wavelength), the SWR does not exceed 1.11. Figure 13 shows the frequency characteristic of the modulus of the reflection coefficient S_{11} for the external Huygens cube, from which we see that, up to the frequency of 30 GHz, the reflectance is below –25.7 dB. With a further increase in the frequency above 150 GHz (more than half a wavelength), non-quasi-static effects begin to manifest themselves; the SWR in this case increases. However, as we see from Figs. 12 and 13, the increase is very small and does not exceed –20.7 dB.

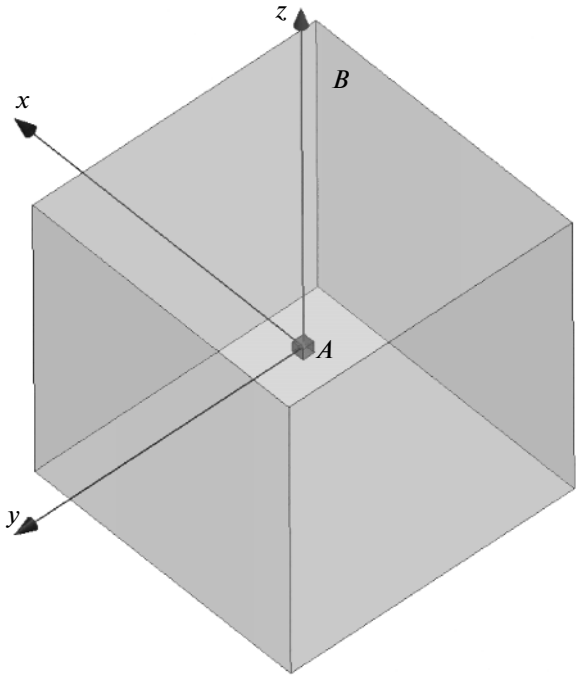

Fig. 10. Geometry of the problem for the external Huygens cube in the ANSYS HFSS v.15 code.

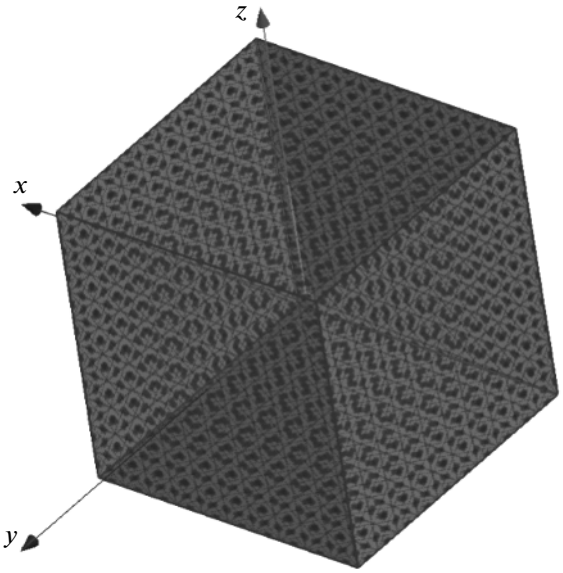

Fig. 11. Absorption (radiation) boundary conditions on the faces of the air cube *B*.

Figure 14 shows the frequency characteristic of attenuation, $L = 10\log|S_{12}|^2$ for the external Huygens cube [1]. Up to the frequency of 17 GHz, the loss on the energy transmission from the first input to the second input is very small and does not exceed –0.08 dB. Then the loss increases. At a quarter-wavelength (75 GHz), it comprises –5.5 dB, at a half-wavelength (150 GHz), –14.4 dB, and, at one wavelength (300 GHz), –40 dB. The extremum of the loss is found at the frequency of 280 GHz and comprises –66.3 dB. The increase in the loss with increasing frequency is connected with the radiation of energy to the external space.

Figure 15 shows the frequency dependence of the gain factor K_a for the external Huygens cube. As we see from the plot, starting from the frequency of 1 GHz (1/300 of the wavelength), K_a increases from –71.64 to –24 dB at the frequency of 10 GHz (1/30 of the wavelength). With further increase in frequency to 15 GHz, K_a increases to –15 dB (1/60 of the wavelength). At the frequency of 28 GHz (7/75 of the wavelength), K_a is –6 dB; at the frequency 30 GHz (1/10 of the wavelength), K_a is –3 dB, and at the frequency of 40 GHz (10/75 of the wavelength), K_a is 0 dB. With further increase in frequency to 55 GHz (11/60 of the wavelength), K_a increases to 3 dB and, at the frequency of 176 GHz (44/75 of the wavelength), K_a reaches 9 dB. Then K_a gradually increases to 12.91 dB at the frequency of 300 GHz (one wavelength).

The frequency characteristic of the phase φ of the transmission coefficient is presented in Fig. 16. This characteristic can be used for constructing the frequency characteristic of the delay, which is shown in Fig. 17. For constructing this characteristic, we use the following formula:

$$\Delta t = \frac{\arg S_{12}}{2\pi f}, \quad (1)$$

where Δt is the delay in seconds, $\arg S_{12}$ is the phase of the transmission coefficient calculated by the ANSYS HFSS v.15 [4] code in radians, and f is the frequency in hertzs.

As we see from Fig. 17, the delay of a signal passing through the external Huygens cube from the first input to the second input as the frequency increases from 1 GHz to 35 GHz increases from 7.3 ps to 7.6 ps. From the frequency of 35 GHz to 150 GHz, the delay decreases from 7.6 ps to 6.4 ps. From the frequency of 150 GHz to 280 GHz, the delay decreases from 6.4 ps to 5.7 ps. After 280 GHz, the delay abruptly decreases almost to zero. Apparently, it is connected with the resonance character of attenuation, which is observed near the frequency of 280 GHz in Fig. 13. After 280 GHz, the phase calculated by the ANSYS HFSS v.15 code should be increased by 2π, so the delay t will be greater rather than smaller. It should be noted that, even for the quasi-static cases, when frequency tends to zero, the delay does not decrease to zero but tends to a constant equal to 7.3 ps. This phenomenon reflects the fact that the phase velocity is independent of frequency.

It is also interesting to plot the dependence of the energy going to radiation. This can be done as follows.

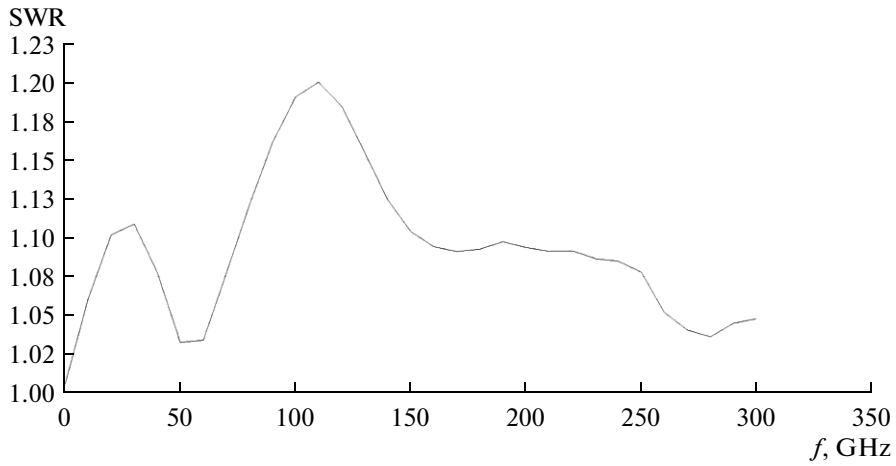

Fig. 12. Frequency characteristic of the SWR for the external Huygens cube in a 25 × 25 × 25 mm air box.

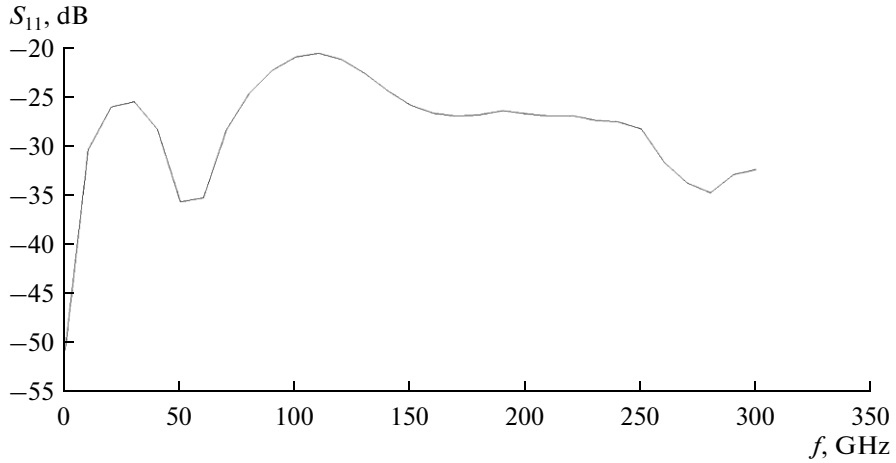

Fig. 13. Frequency characteristic of the reflection coefficient S_{11} for the external Huygens cube in a 25 × 25 × 25 mm air box.

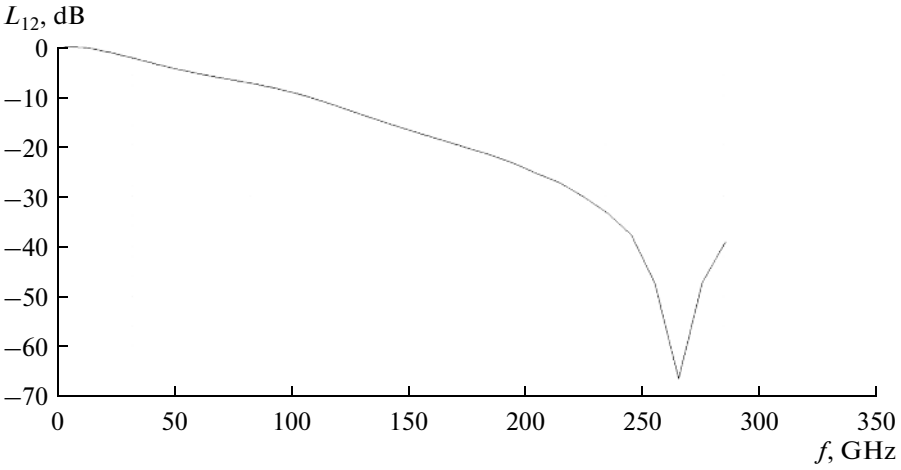

Fig. 14. Frequency characteristic of the attenuation L_{12} for the external Huygens cube in a 25 × 25 × 25 mm air box.

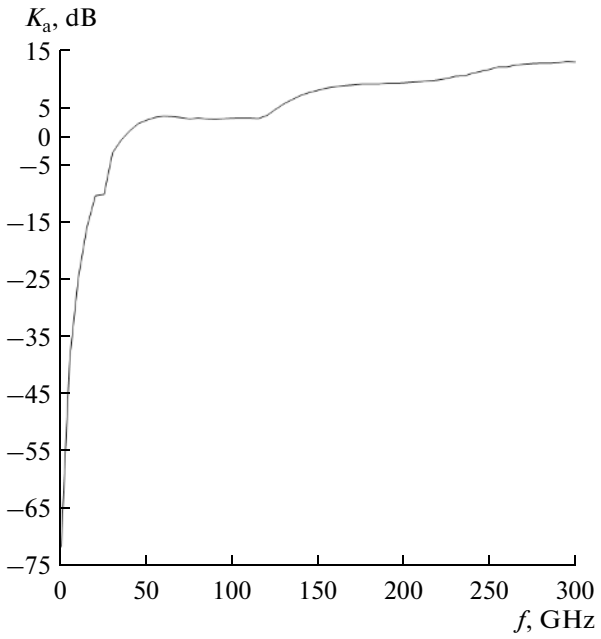

Fig. 15. Frequency characteristic of the gain factor K_a for the external Huygens cube in a 25 × 25 × 25 mm air box.

Since the moduli of the transmission ($|S_{12}|$) and reflection ($|S_{11}|$) coefficients, being squared, represent the power of the signal passing to the second input and reflected to the first input, the power of the signal radiated to the external space is determined by the expression

$$P_{rad} = 1 - (|S_{11}|^2 + |S_{12}|^2) \quad (2)$$

or

$$P_{rad}(\text{dB}) = 10\log(1 - (|S_{11}|^2 + |S_{12}|^2)). \quad (3)$$

Figure 18 shows the plot of the dependence of P_{rad} on the frequency f. As we see from the plot, up to the frequency of 21 GHz, P_{rad} is undefined because it is smaller than zero. This result is explained by the inaccuracy of computations by the ANSYS HFSS v.15 code. Starting from the frequency of 21 GHz, P_{rad} increases from −20.8 dB to −6 dB (40 GHz, which corresponds to the side of the external Huygens cube of 2/15 of the wavelength), −3 dB (55 GHz, which corresponds to the side of the external Huygens cube of 11/60 of the wavelength), −1.76 dB (75 GHz, which corresponds to the side of the external Huygens cube of 1/4 of the wavelength), −0.5 dB (150 GHz, which corresponds to the side of the external Huygens cube of 1/2 of the wavelength), −0.36 dB (225 GHz, which corresponds to the side of the external Huygens cube of 3/4 of the wavelength), and −0.1 dB (300 GHz, which corresponds to the side of the external Huygens cube of one wavelength).

Thus, using the ANSYS HFSS v.15 code [4], we performed the numerical simulation of the frequency characteristics of the external Huygens cube in an air box with the dimensions of 25 × 25 × 25 mm.

3. ANALYSIS OF THE CONVERGENCE OF THE CHARACTERISTICS OF THE EXTERNAL HUYGENS CUBE AS A FUNCTION OF THE SIZE OF THE AIR BOX

The results presented above were obtained by the numerical simulation of the characteristics of the external Huygens cube with the side of the air box B (see Fig. 10) of 25 mm.

Let us calculate the characteristics of the external Huygens cube with the sides of the air box B of 10 and 5 mm and compare the results with the results presented above. Thus we will study the convergence of

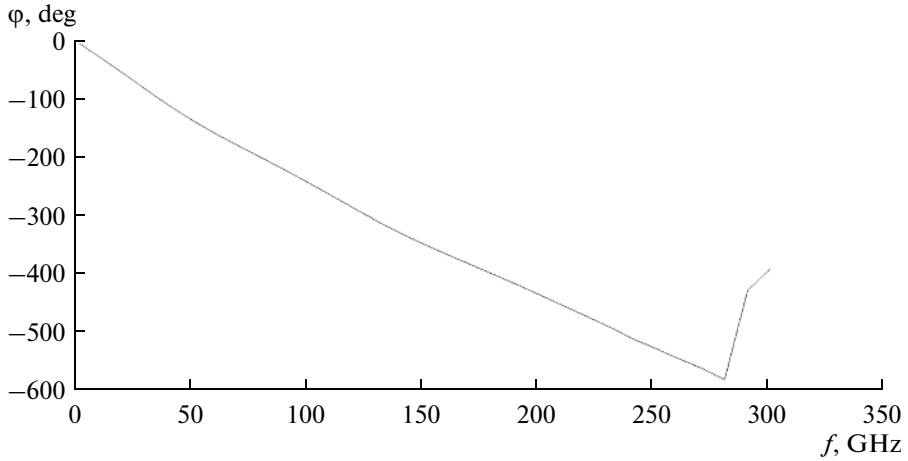

Fig. 16. Frequency characteristic of the phase φ of the transmission coefficient for the external Huygens cube in a 25 × 25 × 25 mm air box.

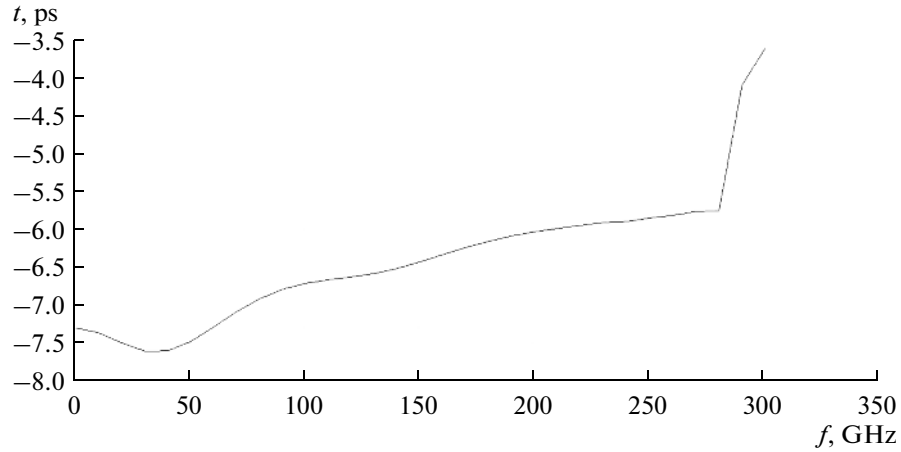

Fig. 17. Frequency characteristic of the delay t of the signal passing to the second input of the external Huygens cube in a 25 × 25 × 25 mm air box.

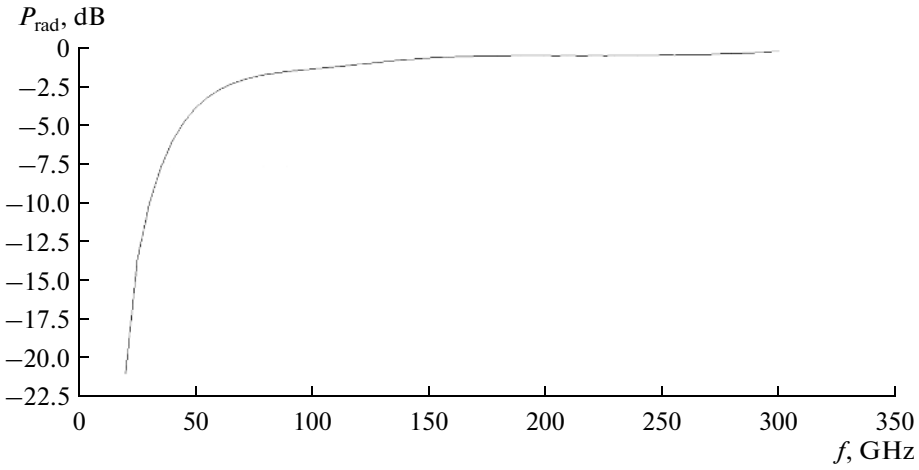

Fig. 18. Frequency characteristic of P_{rad} for the external Huygens cube in a 25 × 25 × 25 mm air box.

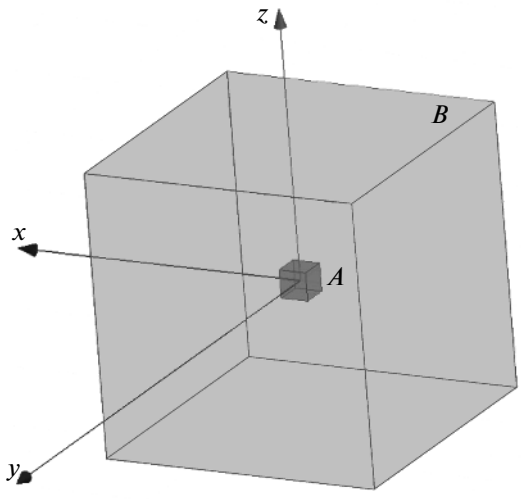

Fig. 19. Geometry of the external Huygens cube with the dimensions 10 × 10 × 10 mm.

the characteristics of the external Huygens cube as a function of the sizes of the air box B.

Let us take an air box B with the dimensions 10 × 10 × 10 mm (Fig. 19).

The simulation was performed in a frequency range from 1 to 300 GHz with a step of 5 GHz. The convergence in the moduli of the scattering matrix Delta S was 0.02, the total number of tetrahedra was 103911, the size of the resulting matrix was 666076, and the required storage was 4.35 GB. The total computation time on a server with two Intel Xeon E5-2690 processors with the frequency of 2.90 GHz and 128 GB RAM was 6 h 24 min 06 s.

The characteristics of the external Huygens cube with the sides 10 × 10 × 10 mm were calculated as in the previous case. Figure 20 shows the frequency characteristic of SWR for the external Huygens cube. Near the frequency of 1 GHz, the side of the considered external Huygens cube was of 1/300 of the wavelength. Starting from the frequency of 30 GHz, which corre-

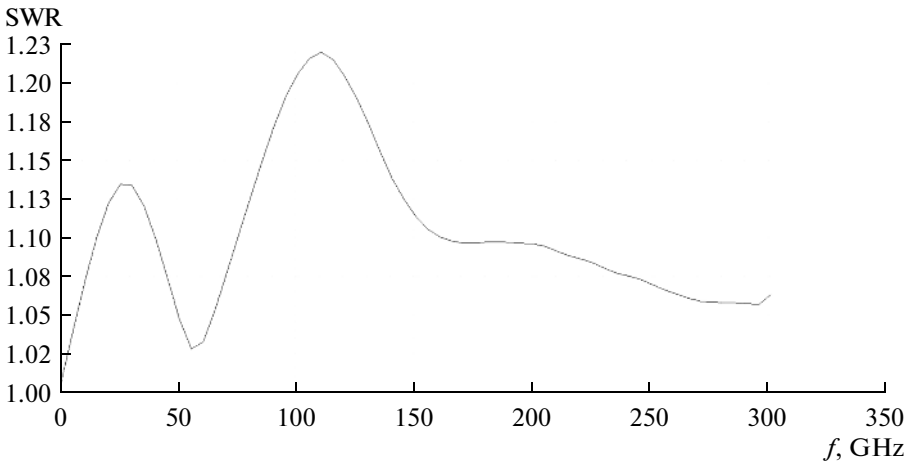

Fig. 20. Frequency characteristic of the SWR for the external Huygens with the dimensions 10 × 10 × 10 mm.

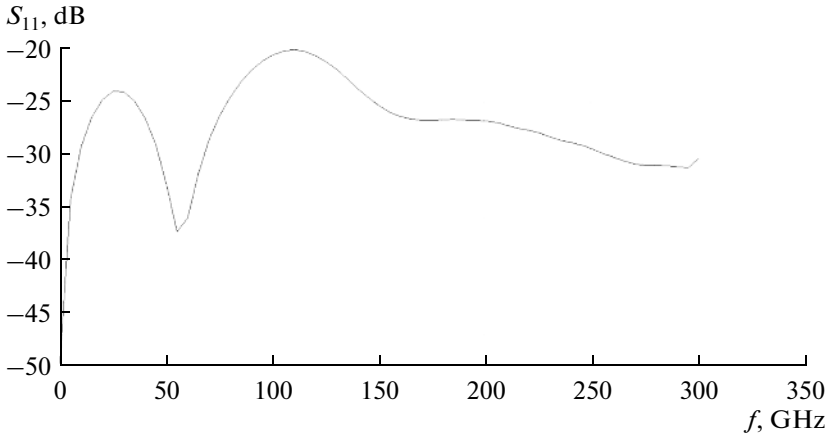

Fig. 21. Frequency characteristic of the reflection coefficient S_{11} for the external Huygens cube with the dimensions 10 × 10 × 10 mm.

sponds to the side of the external Huygens cube of 1/10 of the wavelength, the static components are not sufficient for describing the phenomena inside the cube. Up to the frequency of 30 GHz (less than 1/10 of the wavelength), the SWR does not exceed 1.13. Figure 21 shows the frequency characteristic of the modulus of the reflection coefficient S_{11} for the external Huygens cube, from which we see that, up to the frequency of 30 GHz, the reflectance is below −24.06 dB. With further increase in the frequency above 150 GHz (more than half a wavelength), non-quasi-static effects begin to manifest themselves and the SWR in this case increases. However, as we see from Figs. 20 and 21, this increase is very small and does not exceed −20.04 dB.

Figure 22 shows the frequency characteristic of attenuation, $L = 10\log|S_{12}|^2$, for the external Huygens cube. Up to the frequency of 17 GHz, the loss on the energy transmission from the first input to the second input is very small and does not exceed −0.09 dB. Further on, the loss increases. At 1/4 of the wavelength (75 GHz), it comprises −5.62 dB; at 1/2 of the wavelength (150 GHz), −14.22 dB; and, at one wavelength (300 GHz), −40.45 dB. The extremum of the loss is found at the frequency of 281 GHz and comprises −68.78 dB. The increase in the loss with increasing frequency is connected with the radiation of energy to the external space.

Figure 23 shows the frequency dependence of the gain factor K_a for the external Huygens cube. As we see from the plot, starting from the frequency of 1 GHz (1/300 of the wavelength), K_a increases from −71.67 to −29 dB at the frequency of 10 GHz (1/30 of the wavelength). With further increase in frequency to 26 GHz (13/150 of the wavelength), K_a increases to −10 dB. At the frequency of 33 GHz (11/100 of the wavelength), K_a is −6 dB; at the frequency of 38 GHz (19/150 of the wavelength), K_a is −3 dB; and, at the frequency of 50 GHz (1/6 of the wavelength), K_a is 0 dB. With fur-

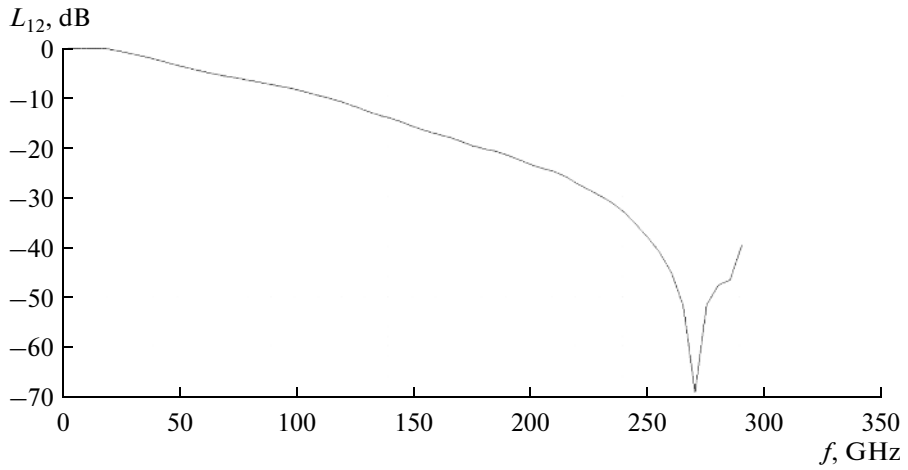

Fig. 22. Frequency characteristic of the attenuation L_{12} for the external Huygens cube with the dimensions 10 × 10 × 10 mm.

ther increase in frequency to 66 GHz (33/100 of the wavelength), K_a increases to 3 dB and, at the frequency of 246 GHz (123/150 of the wavelength), K_a reaches 9 dB. Then K_a gradually increases to 10.63 dB at the frequency of 300 GHz (one wavelength).

The frequency characteristic of the phase of the transmission coefficient is presented in Fig. 24. This characteristic can be used for constructing the frequency characteristic of the delay, which is shown in Fig. 25. For constructing this characteristic, we use formula (1).

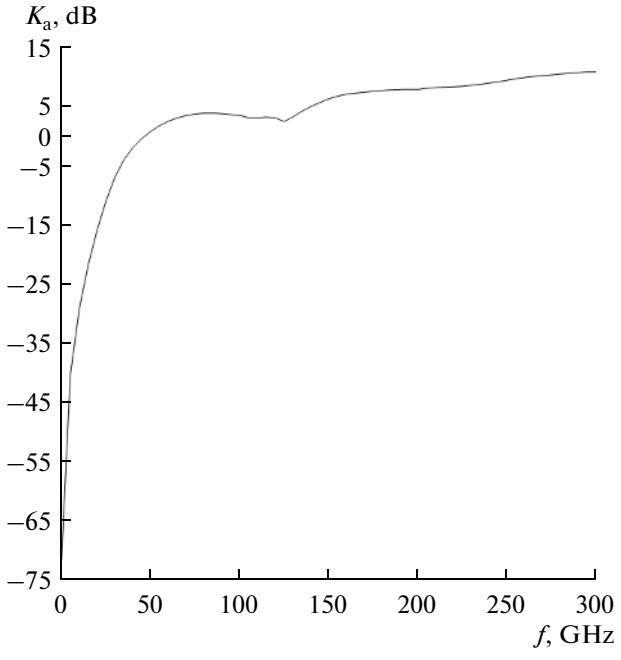

Fig. 23. Frequency characteristic of the gain factor K_a for the external Huygens cube with the dimensions 10 × 10 × 10 mm.

As we see from Fig. 25, the absolute value of delay of a signal passing through the external Huygens cube from the first input to the second input with the frequency increasing from 1 GHz to 35 GHz increases from 7.31 ps to 7.62 ps. As the frequency increases from 35 GHz to 150 GHz, the absolute value of the delay decreases from 7.62 ps to 6.4 ps. With a further increase in frequency from 150 GHz to 275 GHz, the absolute value of the delay decreases from 6.4 ps to 5.77 ps. After the frequency of 275 GHz, the delay abruptly decreases practically to zero. Apparently, it is connected with the resonance character of attenuation, which is observed near the frequency of 281 GHz in Fig. 21. After the frequency of 280 GHz, the phase calculated by the ANSYS HFSS v.15 code [4] should be increased by 2π, so the delay will be greater rather than smaller. It should be noted that, even for the quasi-static cases, when frequency tends to zero, the delay does not decrease to zero but tends to a constant equal to 7.44 ps.

Figure 26 shows the plot of the dependence of the energy going to radiation, P_{rad}, on the frequency f on the basis of relationships (2) and (3) for the external cube B with the dimensions 10 × 10 × 10 mm. As we see from the plot, up to the frequency of 21 GHz, P_{rad} is undefined because it is smaller than zero. This result is explained by the inaccuracy of computations by the ANSYS HFSS v.15 code [4]. Starting from the frequency of 21 GHz, P_{rad} increases from −23.93 dB to −6 dB (40 GHz, which corresponds to the edge of the external Huygens cube of 2/15 of the wavelength), −3.18 dB (55 GHz, which corresponds to the edge of the external Huygens cube of 11/60 of the wavelength), −1.71 dB (75 GHz, which corresponds to the edge of the external Huygens cube of 1/4 of the wavelength), −0.5 dB (150 GHz, which corresponds to the edge of the external Huygens cube of 1/2 of the wavelength), −0.36 dB (225 GHz, which corresponds to the edge of the external Huygens cube of 3/4 of the

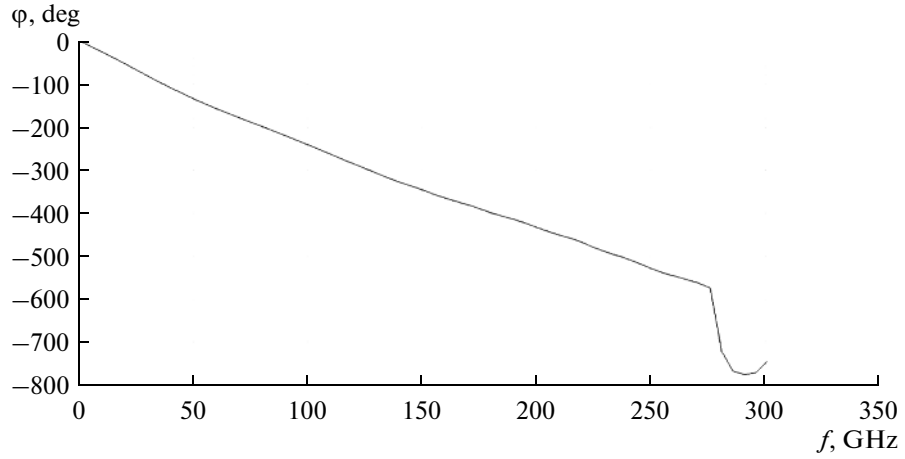

Fig. 24. Frequency characteristic of the phase φ of the transmission coefficient for the external Huygens cube with the dimensions 10 × 10 × 10 mm.

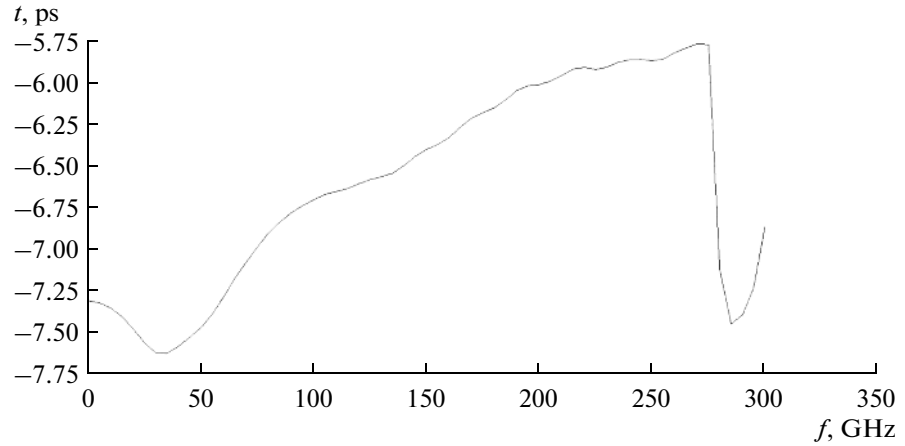

Fig. 25. Frequency characteristic of the delay t of the signal passing to the second input of the external Huygens cube with the dimensions 10 × 10 × 10 mm.

wavelength), and –0.1 dB (300 GHz, which corresponds to the edge of the external Huygens cube of one wavelength).

Now let us consider an air cube B with the dimensions of 5 × 5 × 5 mm (Fig. 27).

The calculation was performed in a frequency range from 1 to 300 GHz with a step of 5 GHz. The convergence in the moduli of the scattering matrix Delta S was 0.02, the total number of tetrahedra was 17266, the size of the resulting matrix was 109330, and the required storage was 434 MB. The total computation time on a server with two Intel Xeon E5-2690 processors with the frequency of 2.90 GHz and 128 GB RAM was 15 min 29 s.

Figure 28 shows the frequency characteristic of SWR for the external Huygens cube with the dimensions 5 × 5 × 5 mm. Near the frequency of 1 GHz, the side of the considered external Huygens cube was of 1/300 of the wavelength. It is the quasi-static case. Starting from the frequency of 30 GHz, which corresponds to the side of the external Huygens cube of 1/10 of the wavelength, the static components are not sufficient for describing the phenomena inside the cube. Up to the frequency of 30 GHz (less than 1/10 of the wavelength), the SWR does not exceed 1.15. Figure 29 shows the frequency characteristic of the modulus of the reflection coefficient S_{11} for the external Huygens cube, from which we see that, up to the frequency of 30 GHz, the reflectance is below –22.63 dB. With a further increase in the frequency above 150 GHz (more than half a wavelength), non-quasi-static effects begin to manifest themselves and the SWR in this case increases. However, as we see from Figs. 27 and 28, this increase is very small and does not exceed –19.56 dB.

Figure 30 shows the frequency characteristic of attenuation, $L = 10\log|S_{12}|^2$, for the external Huygens cube. Up to the frequency of 17 GHz, the loss on the

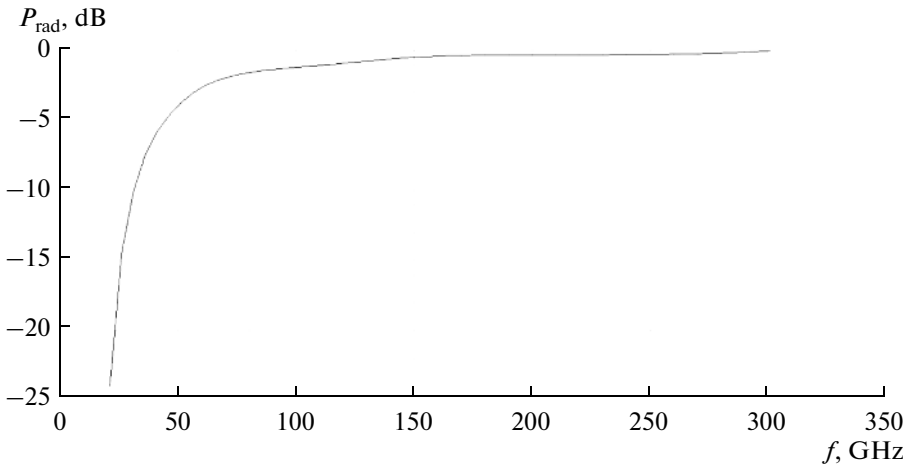

Fig. 26. Frequency characteristic of P_{rad} for the external Huygens cube with the dimensions $10 \times 10 \times 10$ mm.

energy transmission from the first input to the second input is very small and does not exceed −0.2 dB. Then the loss increases. At 1/4 of the wavelength (75 GHz), it comprises −5.25 dB; at 1/2 of the wavelength (150 GHz), −14.5 dB; and, at one wavelength (300 GHz), −41.79 dB. The extremum of the loss is found at the frequency of 280 GHz and comprises −58 dB. The increase in the loss with increasing frequency is connected with the radiation of energy to the external space.

Figure 31 shows the frequency dependence of the gain factor for the external Huygens cube. As we see from the plot, starting from the frequency of 1 GHz (1/300 of the wavelength), K_a increases from −61.98 to −20 dB at the frequency of 10 GHz (1/30 of the wavelength). With further increase in frequency to 21 GHz (7/100 of the wavelength), K_a increases to −11.09 dB. At the frequency of 27 GHz (27/300 of the wavelength), K_a is −6 dB; at the frequency of 35 GHz (7/60 of the wavelength), K_a is −3 dB; and, at the frequency of 50 GHz (1/6 of the wavelength), K_a is 0 dB. With further increase in frequency to 125 GHz (25/60 of the wavelength), K_a increases to 3 dB. After that K_a increases to 9 dB at the frequency of 240 GHz (48/60 of the wavelength). Then K_a gradually increases to 11.39 dB at the frequency of 300 GHz (one wavelength).

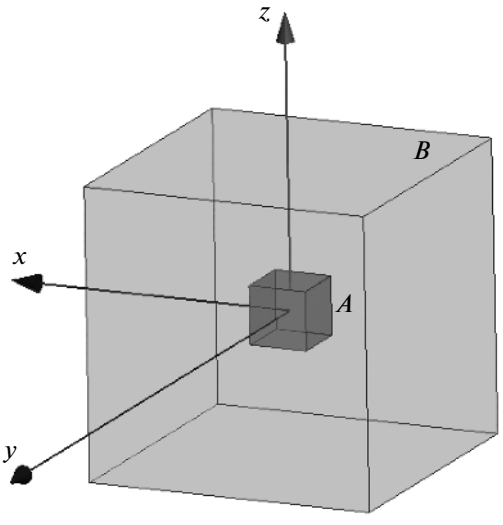

Fig. 27. Geometry of the external Huygens cube with the dimensions $5 \times 5 \times 5$ mm.

The frequency characteristic of the phase φ of the transmission coefficient is presented in Fig. 32. This characteristic can be used for constructing the frequency characteristic of the delay, which is shown in Fig. 33. For constructing this characteristic, we use formula (1).

As we see from Fig. 33, the absolute value of the delay of a signal passing through the external Huygens cube from the first input to the second input with the frequency increasing from 1 GHz to 43 GHz increases from 7.41 ps to 7.5 ps. As the frequency increases from 43 GHz to 150 GHz, the absolute value of the delay decreases from 7.5 ps to 6.43 ps. With further increase in frequency from 150 GHz to 275 GHz, the absolute value of the delay decreases from 6.43 ps to 5.43 ps. After the frequency of 275 GHz, the delay sharply increases, although, as was observed in the previous plots, it must decrease. Apparently, it is a result of computation error of the ANSYS HFSS v.15 code applied to the Huygens cube with the side of 5 mm. The abrupt variation in the curve, apparently, is connected with the resonant character of attenuation, which is observed near the frequency of 280 GHz in Fig. 20. After the frequency of 280 GHz, the phase calculated by the ANSYS HFSS v.15 code [4] should be increased by 2π, so the delay will be greater rather than smaller. It should be noted that, even for the

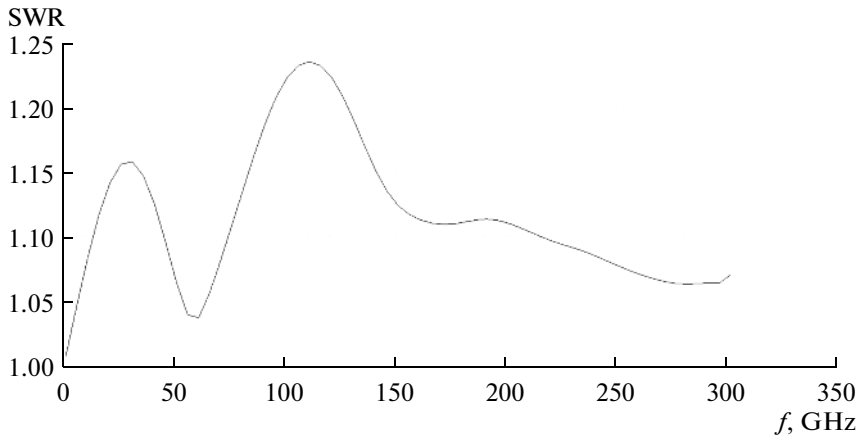

Fig. 28. Frequency characteristic of the SWR for the external Huygens with the dimensions 5 × 5 × 5 mm.

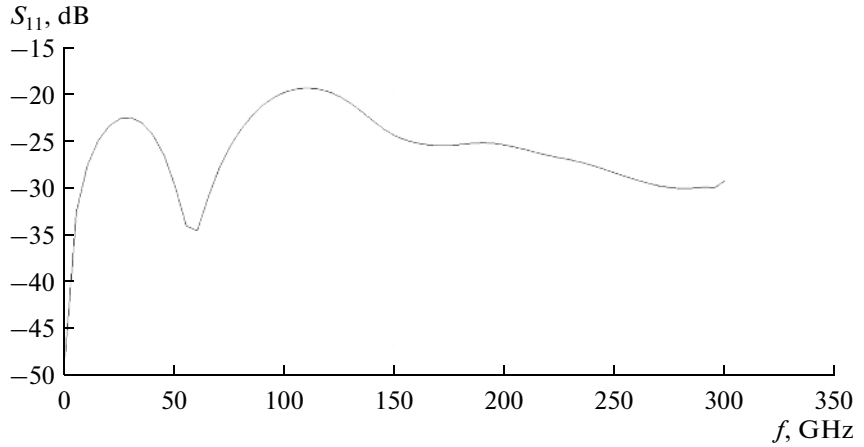

Fig. 29. Frequency characteristic of the reflection coefficient S_{11} for the external Huygens cube with the dimensions 5 × 5 × 5 mm.

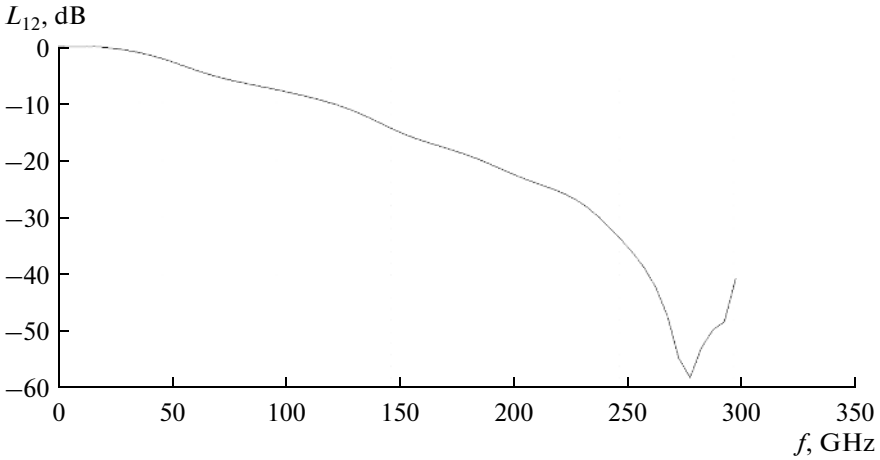

Fig. 30. Frequency characteristic of the attenuation L_{12} for the external Huygens cube with the dimensions 5 × 5 × 5 mm.

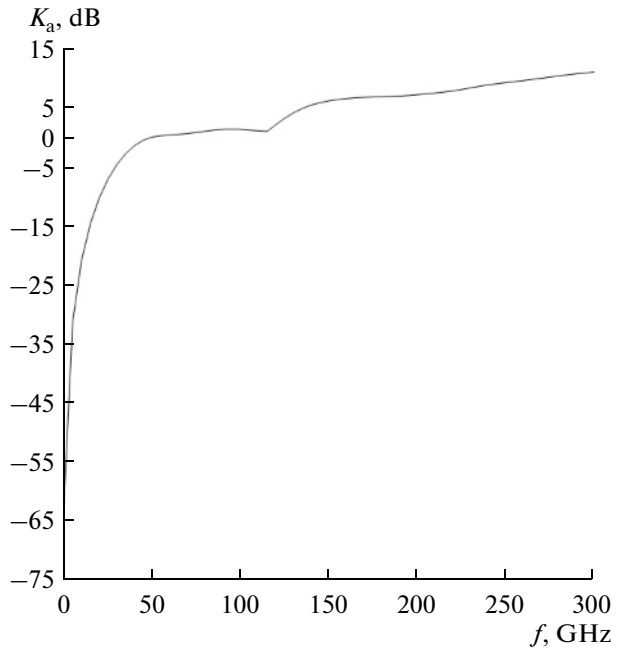

Fig. 31. Frequency characteristic of the gain factor K_a for the external Huygens cube with the dimensions 5 × 5 × 5 mm.

quasi-static cases, when frequency tends to zero, the delay does not decrease to zero but tends to a constant equal to 7.4 ps.

Now let us plot of the frequency dependence of the energy going to radiation, on the basis of relationships (2) and (3) for the external cube *B* with the dimensions 5 × 5 × 5 mm.

Figure 34 shows the plot of P_{rad} versus the frequency *f* for the external cube *B* with the dimensions 5 × 5 × 5 mm. As we see from the plot, up to the frequency of 10.5 GHz, P_{rad} is undefined because it is smaller than zero. It is connected with the inaccuracy of computations by the ANSYS HFSS v.15 code [4]. Starting from the frequency of 10.5 GHz, P_{rad} increases from −28.5 dB to −6.75 dB (40 GHz, which corresponds to the edge of the external Huygens cube of 2/15 of the wavelength), −3.32 dB (55 GHz, which corresponds to the edge of the external Huygens cube of 11/60 of the wavelength), −1.71 dB (75 GHz, which corresponds to the edge of the external Huygens cube of 1/4 of the wavelength), −0.48 dB (150 GHz, which corresponds to the edge of the external Huygens cube of 1/2 of the wavelength), −0.34 dB (225 GHz, which corresponds to the edge of the external Huygens cube of 3/4 of the wavelength), and −0.1 dB (300 GHz, which corresponds to the edge of the external Huygens cube of one wavelength).

The characteristics presented above were calculated for the external Huygens cube with the side of the air cube *B* of 5 mm (Fig. 27).

For validation of the numerical results presented above, we compared the results of calculation of the characteristics of an external Huygens cube with the sides of the air cube *B* of 5, 10, and 25 mm.

4. COMPARISON OF THE CHARACTERISTICS OF EXTERNAL HUYGENS CUBES WITH THE SIDES OF THE AIR CUBE *B* OF 5, 10, AND 25 mm

Figure 35 shows the frequency characteristics of the SWR for external Huygens cubes with the sides of the air cube *B* of 5, 10, and 25 mm (curves *1*–*3*).

Figure 36 shows the frequency characteristics of the moduli of the reflection coefficients S_{11} for external Huygens cubes with the sides of the air cube *B* of 5, 10, and 25 mm (curves *1*–*3*).

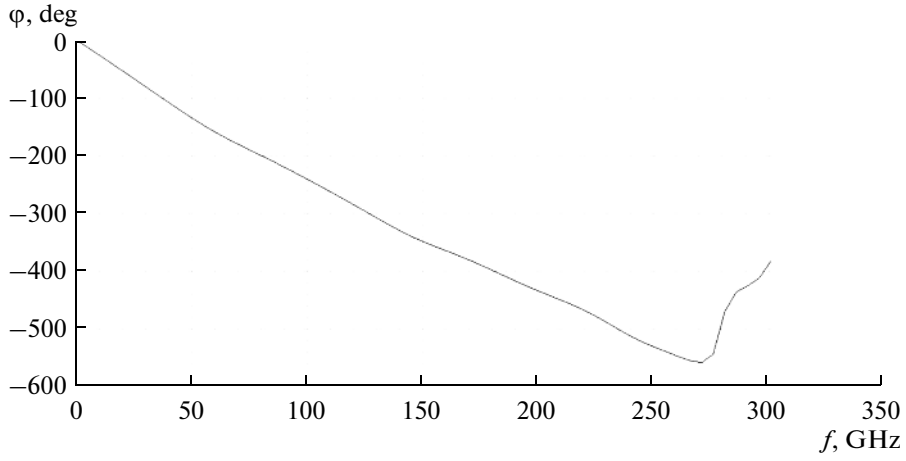

Fig. 32. Frequency characteristic of the phase φ of the transmission coefficient for the external Huygens cube with the dimensions 5 × 5 × 5 mm.

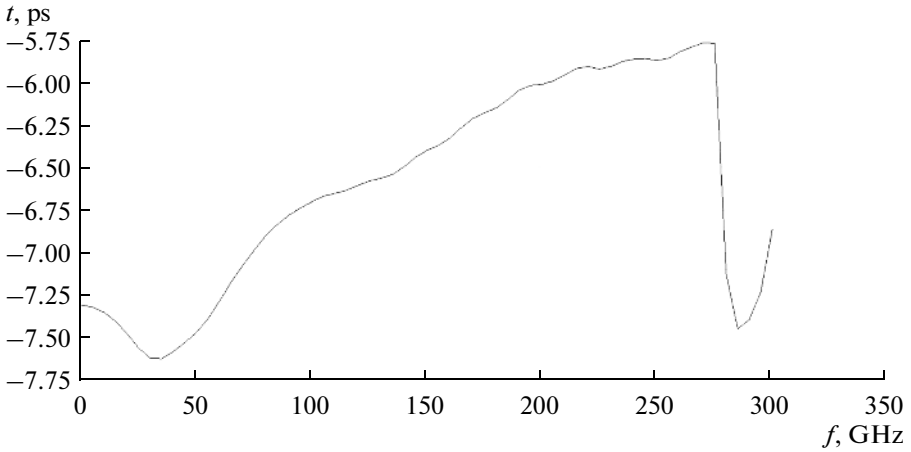

Fig. 33. Frequency characteristic of the delay t of the signal passing to the second input of the external Huygens cube with the dimensions $5 \times 5 \times 5$ mm.

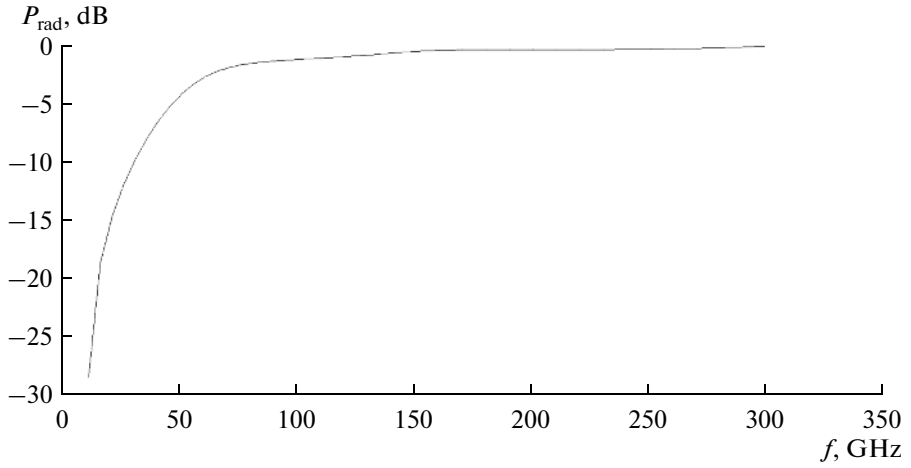

Fig. 34. Frequency characteristic of P_{rad} for the external Huygens cube with the dimensions $5 \times 5 \times 5$ mm.

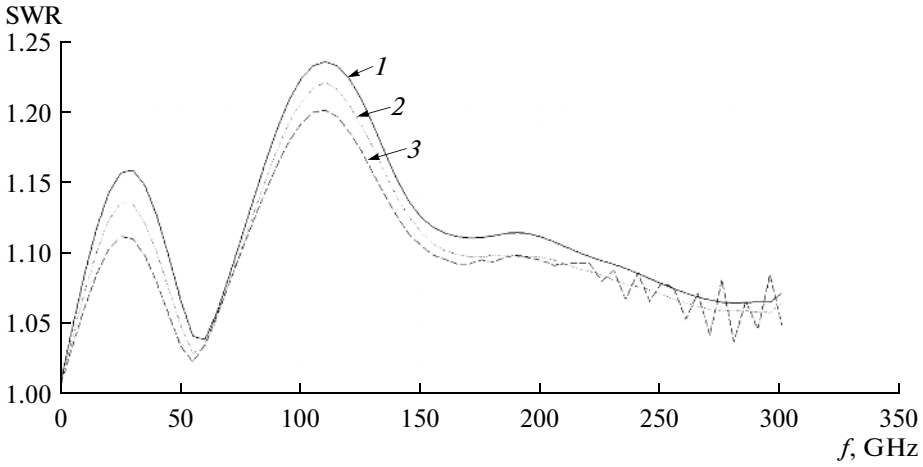

Fig. 35. Frequency characteristic of the SWR for the external Huygens with side of the air cube B of (*1*) 5, (*2*) 10, and (*3*) 25 mm.

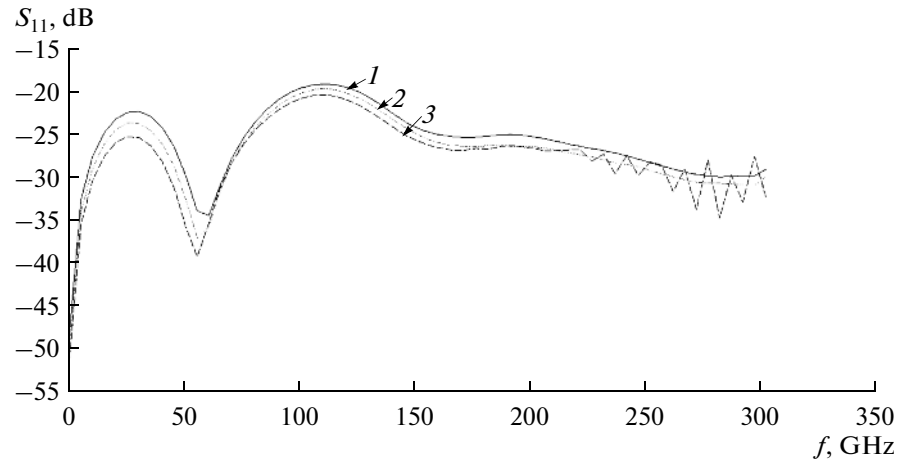

Fig. 36. Frequency characteristic of the reflection coefficient S_{11} for the external Huygens cubes with the side of the air cube B of (*1*) 5, (*2*) 10, and (*3*) 25 mm.

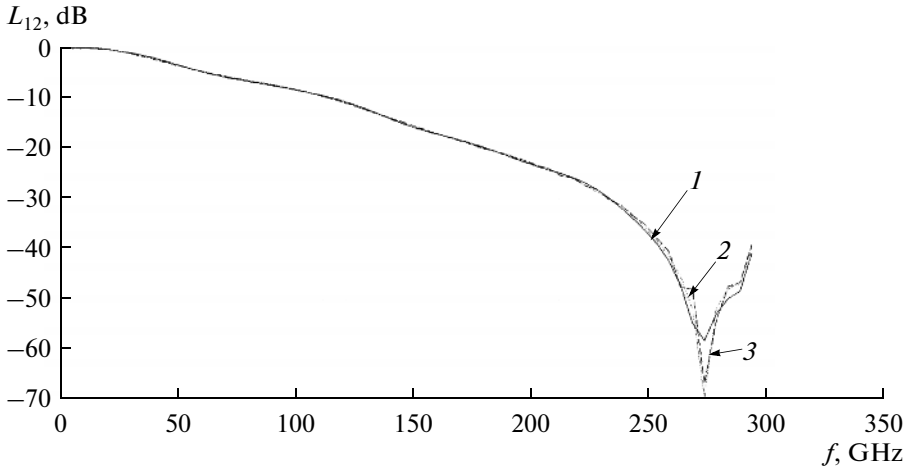

Fig. 37. Frequency characteristic of the attenuation L_{12} for the external Huygens cubes with the side of the air cube B of (*1*) 5, (*2*) 10, and (*3*) 25 mm.

Figure 37 shows the frequency characteristics of the attenuations L_{12} for external Huygens cubes with the sides of the air cube B of 5, 10, and 25 mm (curves *1*–*3*).

As we see from Figs. 35–37, the differences between the SWR, the moduli of the reflection coefficients, and the attenuations for different sides of the external cube are small.

Now let us consider the dependence on the side of the external Huygens cube of the gain factor K_a, whose theoretical limit is the directivity. For this purpose, we use the following formula, which determines the frequency dependence of the directivity [4]:

$$D = \frac{4\pi S}{\lambda^2}, \tag{4}$$

where D is the directivity at the wavelength for a plane cophased aperture of area S with a uniform feed distribution.

Since this relationship was derived under the assumption that all energy on the aperture is radiated, this relationship is valid for directivity only for an aperture of $\lambda \times \lambda$ (see Figs. 14, 18, 22, 26, 30, 34). For directivity, the losses are disregarded, but they are taken into account in K_a [5]:

$$K_a = \eta D. \tag{5}$$

The assumptions made when deriving relationship (4) are the same as in the determination of the K_a of a radiator in the ANSYS HFSS v.15 code [4]. Taking into account that

$$S = 10^{-3} \times 10^{-3} = 10^{-6}\ \text{m}^2, \tag{6}$$

$$\lambda = \frac{c}{f}, \tag{7}$$

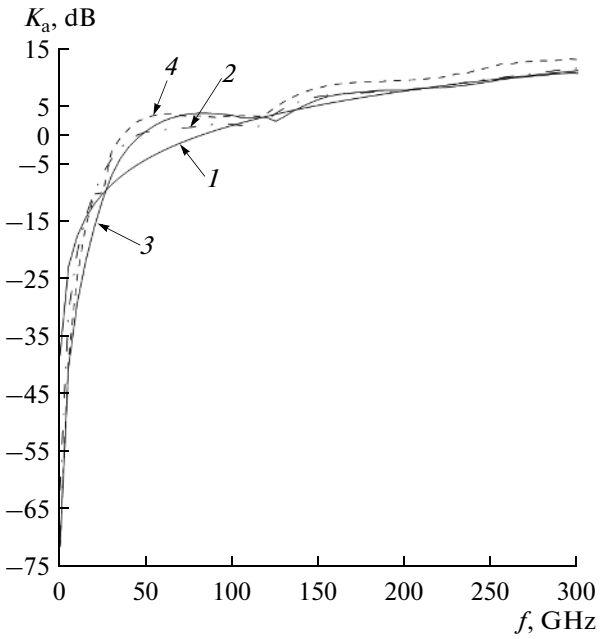

Fig. 38. (*1*) Theoretical and simulated frequency characteristics of the gain factor for the external Huygens cube with the side of the air cube B of (*2*) 5, (*3*) 10, and (*4*) 25 mm.

where $c = 3 \times 10^8$ m/s is the speed of light in vacuum and f is the frequency in hertzs, we obtain the following relationship for the gain factor

$$K_a(\text{dB}) = 10\log\left(\frac{4\pi \times 10^{-6}}{(3\times 10^8)^2} \times (10^9 f')^2\right), \qquad (8)$$

where f' is the frequency in gigahertzs, which we transform to

$$K_a(\text{dB}) = 10\log\left(\frac{4\pi}{9} \times 10^{-4} (f')^2\right) \qquad (9)$$

or

$$K_a(\text{dB}) = k + 20\log f', \qquad (10)$$

where $k = 10\log\left(\frac{4\pi}{9} \times 10^{-4}\right) = -38.55$ dB. At $f' = 1$ GHz, we obtain K_a (dB) $= k = -38.55$ dB.

Frequency dependence (10) of the aperture gain factor K_a is represented by curve *1* in Fig. 38.

Figure 38 also presents plots of the frequency dependence of the gain factor for external Huygens cubes with the sides of the air cube B of 5, 10, and 25 mm (curves *2*–*4*).

Figure 39 shows the frequency characteristics of the phase of the transmission coefficient for external Huygens cubes with the sides of the air cube B of 5, 10, and 25 mm (curves *1*–*3*).

Figure 40 shows the frequency characteristics of the delay t of passage for external Huygens cubes with the sides of the air cube B of 5, 10, and 25 mm (curves *1*–*3*).

Figure 41 shows the frequency characteristics of P_{rad} for external Huygens cubes with the sides of the air cube B of 5, 10, and 25 mm (curves *1*–*3*).

As we see from the plots of the frequency characteristics of the external Huygens cubes shown in Figs. 35–41, in the simulation, a significant reduction in the side of the air cube B from 25 mm to 5 mm is possible. This makes possible a significant reduction in the computation time in the simulation.

5. COMPARISON OF THE SCATTERING MATRICES OF THE INTERNAL AND EXTERNAL HUYGENS CUBES

The external and internal [9] Huygens cubes are four-terminal networks. Let us compare their scatter-

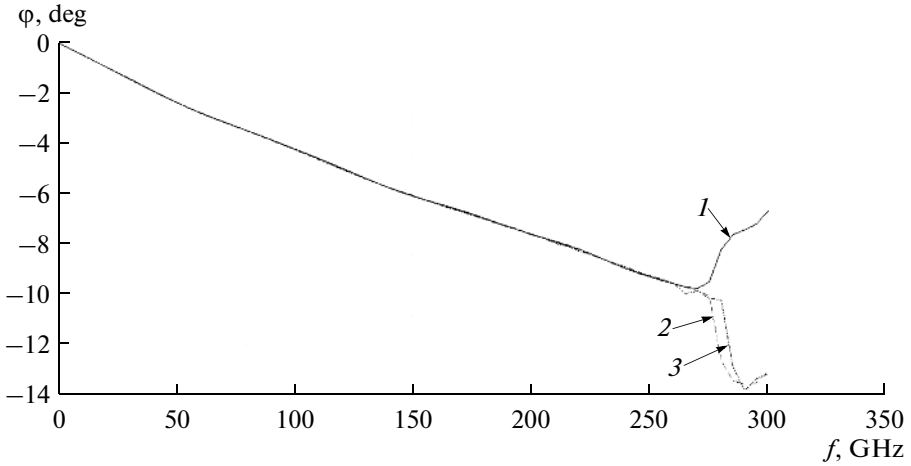

Fig. 39. Frequency characteristic of the phase φ of the transmission coefficient for the external Huygens cube with the sides of the air cube B of (*1*) 5, (*2*) 10, and (*3*) 25 mm.

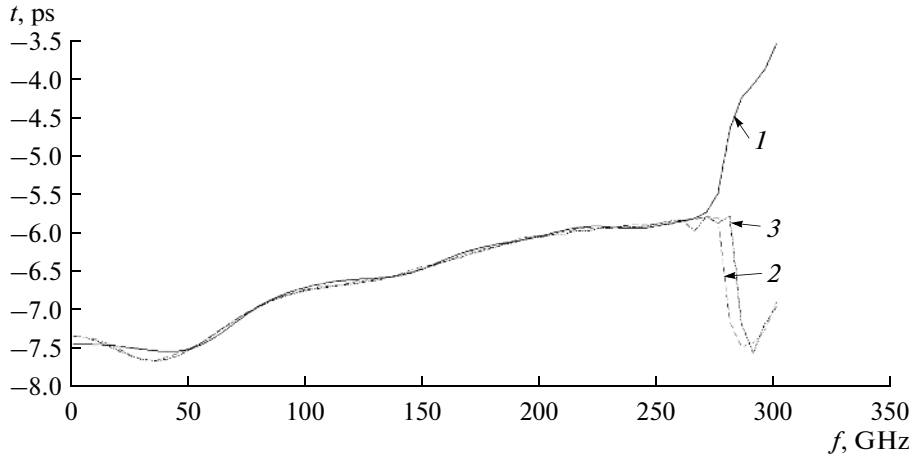

Fig. 40. Frequency characteristic of the delay t of the signal passing to the second input of the external Huygens cube with the sides of the air cube B of (*1*) 5, (*2*) 10, and (*3*) 25 mm.

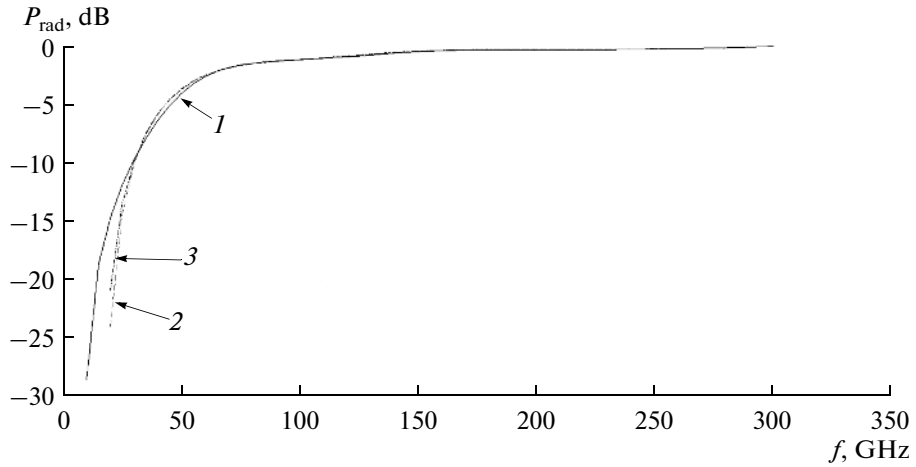

Fig. 41. Frequency characteristic of P_{rad} for the external Huygens cube with the sides of the air cube B of (*1*) 5, (*2*) 10, and (*3*) 25 mm.

ing matrices for the quasi-static case, i.e., at frequencies tending to zero. For numerical calculations, we will make it at the frequency of 1 GHz.

The table presents the comparison of the moduli and phases of the scattering matrices of the internal and external Huygens cubes, which leads to the following conclusion: in the quasi-static case, the external and internal Huygens cubes are similar in the sense that both of them are matched and almost all the energy is transferred from the first input to the second input. They differ in the phase of the transmission coefficient (the phase of S_{12}), i.e., in the delay of the signal passing from the first input to the second input (from the second to the first ones). For the quasi-static case, the external Huygens cube practically does not radiate energy and almost all the energy is transferred from the first input to the second input.

Comparison of the moduli and phases of the scattering matrices of the internal and external Huygens cubes

Frequency characteristics	The value for the internal Huygens cube at the frequency of 1 GHz	The value for the external Huygens cube at the frequency of 1 GHz
$\lvert S_{11}\rvert$, dB	−207.2	−51.1
Phase S_{11}, rad	−0.0482	−1.61
$\lvert S_{12}\rvert$, dB	0	−0.0001
Phase S_{12}, rad	−0.021	−0.046
Delay, ps	−3.33	−7.3

6. THE EXTERNAL HUYGENS CUBE AS A FREQUENCY DIPLEXER

1. It can be said that the external Huygens cube is matched in the whole frequency band, because its

SWR does not exceed 1.25 (see Fig. 35). The corresponding plot of the frequency dependence of the reflection coefficient is shown in Fig. 36, from which we see that the modulus of the reflection coefficient does not exceed –20 dB.

2. The frequency dependence of the attenuation L_{12} of a signal passing from the first input to the second input of the external Huygens cube is as follows (see Fig. 37): for frequencies below 55 GHz (11/60 of the wavelength), L_{12} is above –3 dB and, for frequencies above 55 GHz, L_{12} is below –3 dB.

3. The frequency dependence of the power radiated to the free space, P_{rad}, has the following form: for frequencies below 55 GHz, the power radiated to the free space is below –3 dB and, for frequencies above 55 GHz, the power radiated to the free space is above –3 dB.

The joint fulfillment of conditions 1–3 makes it possible to consider the external Huygens cube as a frequency diplexer [10–12].

CONCLUSIONS

The results of numerical calculation of the frequency characteristics of the external Huygens cube lead to the following conclusions.

(1) The external Huygens cube is matched in the whole frequency band (its SWR does not exceed 1.25).

(2) The fraction of the radiated energy tends to unity when the size of the external Huygens cube equals the wavelength. In this case, K_a tends to 12.91 dB.

(3) For a small Huygens cube (1/15 of the wavelength), the free space acts like a below-cutoff waveguide and energy is not radiated (the radiation loss are higher than –25 dB).

(4) The gain of the external Huygens cube becomes greater than zero when the side of the external Huygens cube become greater than 1/12 of the wavelength.

(5) The external Huygens cube may be considered as a frequency diplexer.

REFERENCES

1. D. M. Sazonov, A. N. Gridin, and B. A. Mishustin, *Microwave Circuits* (Vysshaya Shkola, Moscow, 1981; Mir, Moscow, 1982).
2. K. N. Klimov, D. S. Gezha, and D. O. Firsov-Shibaev, *Practical Application of Electrodynamic Modelling* (Lambert Academic Publishing, Saarbrucken, 2012) [in Russian].
3. K. N. Klimov, D. O. Firsov-Shibaev, and D. S. Gezha, *Method of Impedance Analysis of Electromagnetic Space* (Lambert Academic Publishing, Saarbrücken, 2013) [in Russian].
4. S. E. Bankov and A. A. Kurushin, Zh. Radioelektron., No. 5 (2009); http://jre.cplire.ru/win/library/7/text.pdf
5. G. T. Markov and D. M. Sazonov, *Antennas* (Energiya, Moscow, 1975) [in Russian].
6. S. I. Baskakov, *Bases of Electrodynamics* (Sovetskoe Radio, Moscow, 1973) [in Russian]
7. M. A. Zheksenov and A. S. Petrov, J. Commun. Technol. Electron. **59**, 289 (2014).
8. M. A. Zheksenov and A. S. Petrov, J. Commun. Technol. Electron. **59**, 427 (2014).
9. A. S. Godin, A. B. Tsai, and K. N. Klimov, J. Commun. Technol. Electron. **60**, 436 (2015).
10. O. V. Alekseev, G. A. Groshev, and G. G. Chavka, *Multi-Channel Frequency-Dividing Devices and Their Application* (Radio i Svyaz', Moscow, 1981) [in Russian].
11. A. L. Fel'dshtein and L. R. Yavich, *Synthesis of Two-Port and Four-Port Networks at Microwave Frequencies* (Svyaz', Moscow, 1971) [in Russian].
12. J. L. Altman, *Microwave Circuits* (D. Van Nostrand, New York, 1964; Mir, Moscow, 1969).

Translated by E. Chernokozhin